The Journal of Experimental Biology 203, 725–739 (2000)
Printed in Great Britain © The Company of Biologists Limited 2000
JEB2653

KINEMATICS AND MECHANICS OF GROUND TAKE-OFF IN THE STARLING *STURNIS VULGARIS* AND THE QUAIL *COTURNIX COTURNIX*

KATHLEEN D. EARLS*

Department of Ecology and Evolutionary Biology, Brown University, Providence, RI 02912, USA

*Present address: Department of Ornithology, American Museum of Natural History, Central Park West at 79th Street, New York, NY 10024, USA (e-mail: kearls@amnh.org)

Accepted 8 December 1999; published on WWW 26 January 2000

Summary

The mechanics of avian take-off are central to hypotheses about flight evolution, but have not been quantified in terms of whole-body movements for any species. In this study, I use a combination of high-speed video analysis and force plate recording to measure the kinematics and mechanics of ground take-off in the European starling *Sturnis vulgaris* and the European migratory quail *Coturnix coturnix*. Counter to hypotheses based on the habits and morphology of each species, *S. vulgaris* and *C. coturnix* both produce 80–90 % of the velocity of take-off with the hindlimbs. *S. vulgaris* performs a countermovement jump (peak vertical force four times body weight) followed by wing movement, while *C. coturnix* performs a squat jump (peak vertical force 7.8 times body weight) with simultaneous wing movement. The wings, while necessary for continuing the movement initiated by the hindlimbs and thereafter supporting the body weight, are not the primary take-off accelerator. Comparison with one other avian species in which take-off kinematics have been recorded (*Columba livia*) suggests that this could be a common pattern for living birds. Given these data and the fact that running take-offs such as those suggested for an evolving proto-flier are limited to large or highly specialized living taxa, a jumping model of take-off is proposed as a more logical starting point for the evolution of avian powered flight.

Key words: take-off, flight, European starling, *Sturnis vulgaris*, European migratory quail, *Coturnix coturnix*, kinematics, mechanics, evolution.

Introduction

Take-off is key to all flight. How an animal makes the transition from a surface to the air is critical not only to individual activity and survival, but to the evolution of powered flight from a non-flying ancestor. Unless the wings of birds appeared full-size and fully functional, evolutionary hypotheses need to address the problem of how a small-winged, weakly muscled flier might be able to get into the air, in addition to determining whether it could support itself using its airfoil. Debate about the evolution of flapping flight in birds has been stalled for several years on the question of take-off (for reviews, see Norberg, 1990; Padian and Chiappe, 1998), since ideas of how a proto-flier supports itself in the air are strongly linked to proposals of how it got into the air. Although all hypotheses and scenarios of the evolution of flight from the ground or the trees must deal with this surface-to-air transition, the take-off mechanics of living birds are largely unknown. How the force to initiate take-off is generated is not known for any avian species, nor have the relative roles of the wings and the hindlimbs been assessed. Without some modern baseline, realistic prediction of the behavior of extinct forms is difficult. Given that the hindlimbs of birds do not support the airfoil, are not reduced or lost in the majority of species and are three-element limbs well-suited to the mechanics of jumping (Alexander, 1995), it is likely that they could generate some portion of the acceleration required for take-off.

Previous work has examined the wing mechanics of take-off and vertical flight of the pigeon *Columba livia* with particular attention to kinematics, muscle activity patterns and power output (Brown, 1948; Simpson, 1983; Dial and Biewener, 1993; Gatesy and Dial, 1993). The forces produced against a perch during take-off have been recorded for both *C. livia* (Heppner and Anderson, 1985) and the European starling *Sturnis vulgaris* (Bonser and Rayner, 1996). However, the movements of the wings, body and hindlimbs have yet to be connected to information on force production to provide an overall picture of avian take-off mechanics. The only study that has analyzed the role of all three elements in the take-off of a volant vertebrate species is a recent analysis of the vampire bat *Desmodus rotundus* (Schutt et al., 1997).

In the present study, I use a combination of kinematics and force plate analyses to partition the contribution of the hindlimbs and the wings to take-off. The platform records the forces applied against the ground, directly measuring the contribution of the hindlimbs to take-off acceleration. The total velocity and acceleration of the center of mass can be calculated from kinematic analysis of high-speed video

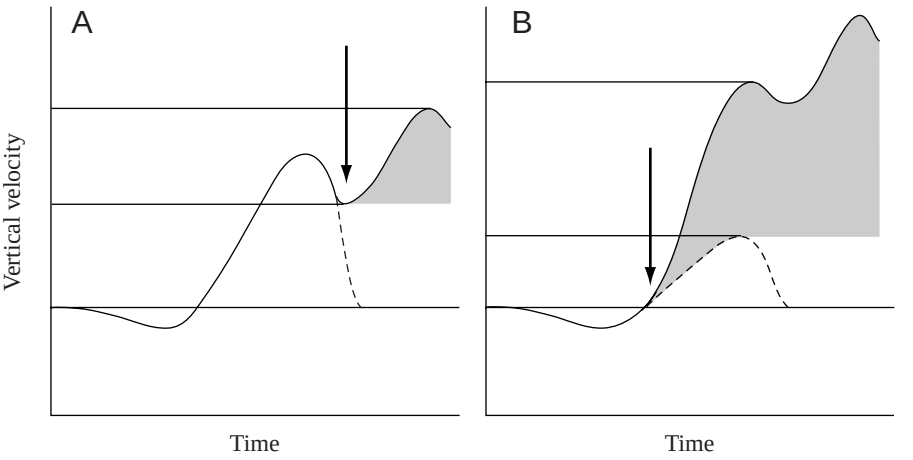

Fig. 1. Alternative hypotheses of vertical velocity generation during take-off. The solid line shows total vertical velocity. The broken line indicates velocity calculated from the force platform data. It would return to zero if the body were to behave ballistically without the action of the wings. The start of downstroke is marked by the arrow. Shading indicates the relative contribution of the wings to take-off; horizontal lines show the increase in vertical velocity resulting from the action of the wings. (A) Hindlimb-driven take-off: predicts sequential action of the wings and the hindlimbs; the velocities calculated from force and video data correspond until the wings begin downstroke. (B) Wing-driven take-off: predicts simultaneous action of the wings and the hindlimbs; the downstroke begins early in take-off, and the contribution of the wings to total velocity is greater than in the hindlimb-driven hypothesis. The contribution of the hindlimbs to vertical velocity is less than in A, and the wings provide a greater proportion of the total velocity.

recordings. Together, these data permit calculation of the contribution of the wings to take-off.

Hypotheses of limb use

If the hindlimbs alone contribute to the bird's initial acceleration, the total vertical velocity calculated from video recordings will correspond to the vertical velocity calculated from the ground reaction force (hindlimb-driven take-off, Fig. 1A). The two velocity curves will diverge after the force produced by the hindlimbs begins to decrease. This divergence is the result of lift production by the wings, which will only appear on the kinematic record. Under these conditions, the contribution of the wings to total take-off velocity will be smaller than that of the hindlimbs. Alternatively, the wings may contribute significantly to velocity prior to lift-off (wing-driven take-off, Fig. 1B). In this model, the wings produce the greater part of the vertical velocity, and the contribution of the hindlimbs will be relatively smaller than in the hindlimb-driven hypothesis.

Since body size, morphology and ecology can all affect take-off behavior, I chose two species that differ in body form and ecology and for which it is possible to formulate testable hypotheses concerning limb use during take-off. The European starling *Sturnis vulgaris* is an arboreal species of disturbed habitats; it mates and raises its young in trees and nests in holes excavated by woodpeckers (Cabe, 1993). Although it forages on the ground, it is not specialized for terrestrial locomotion. *S. vulgaris* walks while on the ground and, when startled, its immediate response is flight rather than running. The wings are relatively long and tapered. Hartman (1961) reported that the musculature of the pectoral extremity comprises 27.5 % of the body mass, and that of the hindlimbs comprises only 7.8 %. Furthermore, the digital flexors, rather than the gastrocnemius, comprise the largest part of the distal leg mass (52 % and 38 %, respectively; K. D. Earls, personal observation), suggesting that grasping ability may be more important than terrestrial locomotion in this species. The relative hindlimb bone proportions of *S. vulgaris* place emphasis on the distal segments of the limb; the femur comprises 26 % of the total limb length, the tibiotarsus 45 % and the tarsometatarsus 29 %.

The European migratory quail *Coturnix coturnix* is a terrestrial specialist of grassland habitats. It spends the majority of its time on the ground and, when threatened, typically runs and hides in dense vegetation rather than flying (Johnsgard, 1988). When *C. coturnix* does fly, its take-off is rapid and is followed by a brief burst of forward flight. Birds soon return to the ground and run to cover. The hindlimbs are large and long, and the wings small and rounded. While the pectoral extremity musculature comprises approximately the same proportion of body mass as in *S. vulgaris* (25.6 %), the pelvic extremity is much larger, the muscles comprising 12 % of the bird's body mass (Hartman, 1961). The thigh musculature is more robust than in *S. vulgaris*, and the digital flexors are a smaller proportion of the leg mass than the gastrocnemius (33 % and 50 %, respectively; K. D. Earls, personal observation). The bone proportions of the hindlimb emphasize the proximal elements; the femur is 33 % of the total limb length, the tibiotarsus 42 % and the tarsometatarsus 25 %. The toes are not modified for grasping, as they are in *S. vulgaris*, and the hallux is smaller than the anterior digits (II, III, IV; K. D. Earls, personal observation).

Given these differences in morphology and habit, take-off from the ground in these two species should differ significantly. I expected *S. vulgaris*, with a largely arboreal lifestyle and relatively small hindlimbs, to generate take-off acceleration primarily with the wings. In contrast, the hindlimbs of *C. coturnix* were expected to produce the majority of take-off acceleration, given its terrestrial habit and large hindlimb musculature. In terms of the vertical velocity predictions in Fig. 1, *S. vulgaris* should perform a wing-driven take-off (Fig. 1B), while *C. coturnix* should use hindlimb-driven take-off (Fig. 1A).

Materials and methods

Animals and training

Adult *Sturnis vulgaris* (mass 77.3±3.7 g; mean ± S.E.M.; *N*=3; range 62.5–86.0 g) were wild-caught and housed in a large cage (1.5 m×1.2 m×0.9 m) in the Brown University Animal Care Facility (ACF). Eight adult *Coturnix coturnix* (mass 172.2±3.9 g; range 168.3–189.2 g) were obtained locally and also housed in the Brown University ACF in a large cage (1.4 m×1.4 m×0.9 m) modified for ground-dwelling birds.

Each *S. vulgaris* was trained for 4–6 weeks to take off from the force plate surface and fly to a rest box for food rewards. The rest box was 4.25 m from the center of the force plate, with an established flight trajectory of 21° to the horizontal. Individuals were either startled with a loud finger snap or took off of their own volition once placed on the plate. This difference in take-off initiation did not appear to alter the behavior or force production of *S. vulgaris* during take-off. *C. coturnix* individuals were repeatedly startled to take off. To ensure take-off rather than other escape behavior by *C. coturnix*, the plate was surrounded on three sides by a 60 cm high cardboard wall. For each trial, an individual was placed under a cover and moved onto the force platform; the cover was then removed, and the animal was startled with a hand-clap or a flapping piece of cloth. All *C. coturnix* were caught in the hand before landing because their flight path was unpredictable.

One to two days prior to data collection, feathers covering anatomical landmarks on the breast, pelvis and hindlimb were removed, following local anesthesia with lidocane. Immediately prior to data collection, reflective tape markers were applied to the breast, synsacrum and hindlimb (Fig. 2A). Because no marker could be placed at the center of mass, I estimated its position as the average of the positions of the breast and synsacrum markers, after curve-fitting (see below for details of curve-fitting).

Twenty-one *S. vulgaris* take-offs, from three individuals, and 19 *C. coturnix* take-offs, from three individuals, were analyzed.

Data collection

Accurate measurement of the relative roles of the wings and the hindlimbs in small birds, using a combined force platform and kinematic method, requires sensitive force platforms, high imaging rates (500–1000 frames s^{-1}) and precise synchronization. Voltage output from a small, table-top force platform (surface dimensions, 25 cm×12 cm; Pharos Systems) was amplified at a calibration of 6 mV g^{-1} (Vishay 2120A; Measurements Group, Inc.). Output from the amplifiers was acquired at 1008 Hz using BioWare (Kistler Instruments Corp.). Simultaneously, all trials were video-taped in lateral view at 1001 frames s^{-1} using a digital camera (KineView 1256p, Adaptive Optics Associates, Inc.) placed 3 m from the center of the force plate. The field of view (35 cm×35 cm) captured the entire plate surface and allowed sufficient vertical and horizontal coverage for one complete wingbeat cycle after lift-off. Force and video data were synchronized using the camera's analog trigger output, which assigns a distinct voltage level to each frame. Digital images were downloaded to video-tape.

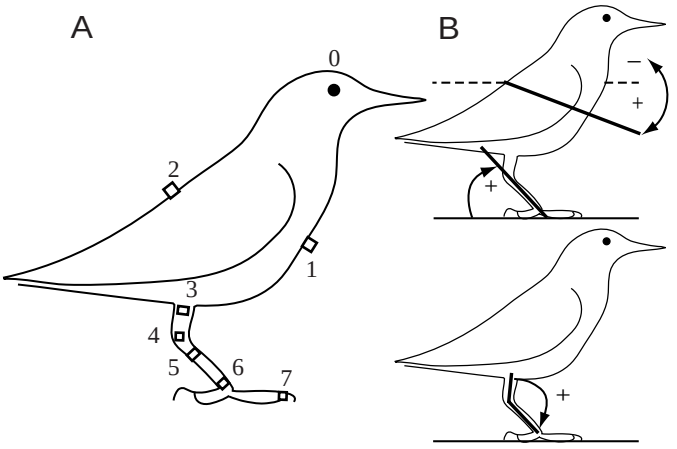

Fig. 2. Digitizing markers and angles used in the kinematic analysis. (A) Digitizing marker positions: 0, eye; 1, breast at anterior end of sternum; 2, midline synsacrum between acetabulae; 3, tibiotarsus below flare of gastrocnemius; 4, center of distal tibiotarsus; 5, proximal tarsometatarsus; 6, distal tarsometatarsus; 7, tip of distal phalanx of digit III. Marker 0 was digitized only in *Coturnix coturnix*. Hindlimb markers were 1 mm wide strips of reflective tape wrapped around the limb. Breast and synsacrum markers were 2×2 mm square tabs of reflective tape over light cardboard, and they projected from the body so they could be seen in lateral view. (B) Angle definitions. Top, body angle is the angle between a line joining the sternum and synsacrum markers (points 1 and 2) and the horizontal. The tarsometatarsus (TMT) angle is the angle between a line connecting the proximal and distal tarsometatarsus markers (points 5 and 6) and the horizontal. Bottom, the intertarsal (IT) angle is delimited by the tibiotarsus, distal tibiotarsus and distal tarsometatarsus markers (points 3, 4 and 6).

Analysis

Definitions

The first wingbeat during take-off is distinct from those that follow (Simpson, 1983) and, from pectoralis muscle force recordings, it seems possible for a bird rapidly to make the transition from take-off to other modes of flight (Dial and Biewener, 1993). For these reasons, I defined take-off as ending with the first upstroke/downstroke transition after lift-off (loss of hindlimb contact with the platform). Take-off, as used in this study, included the unfolding of the wing and the first complete wingbeat cycle (i.e. unfolding, downstroke, upstroke). To compare take-offs accurately among individuals and between species, I designated the *start of take-off* as the time when vertical force reached 105% of body weight, the *end of hindlimb thrust* as the time when vertical force fell to 95% of body weight, and *lift-off* as the time when vertical force fell below 5% of body weight.

Consistent criteria were used to determine kinematic events. The start of wing unfolding was marked as the initial movement of the wing away from the body. In lateral view,

this was perceived as downward movement of the primaries followed immediately by elevation of the proximal wing; the time was noted at the drop of the primaries. Mid-downstroke and mid-upstroke were marked when the wing pointed along the camera's field of view (parallel to the ground). The start of downstroke and upstroke/downstroke transition were the initial separation of the fully extended wings, determined from the movement of the wrist region. The downstroke/upstroke transition was also determined from the movement of the wrist region.

All kinematic and mechanical event times were calculated with reference to the start of take-off. I analyzed force and kinematic data simultaneously, using software for analysis of time series data (Igor Pro, v. 3.12; WaveMetrics Corp.).

Mechanics

Force plate voltage outputs were base-corrected for amplifier offset, smoothed to remove noise using a seven-pass binomial algorithm (attenuation of the signal due to smoothing was less than 3 %) and converted from volts to newtons. Force data from each end of the plate were summed to give total vertical, antero-posterior (horizontal) and medio-lateral (lateral) forces. In most trials, lateral forces were small compared with vertical and horizontal forces (5–14 % vertical) and were therefore omitted from the analysis. Body weight for each individual was calculated from the average of the pre-take-off vertical forces from each day's data collection.

Horizontal and vertical velocity and impulse were integrated from the force data, after body weight had been subtracted from the vertical force. Both velocity and impulse were calculated from the time the force first diverged from body weight until lift-off. For comparison between species, force and impulse were converted from newtons and newton seconds (N s) to multiples of body weight ($\times m\boldsymbol{g}$ and $\times m\boldsymbol{g}$ s, respectively, where m is body mass in kg and $\boldsymbol{g}$ is the acceleration due to gravity) by dividing by the appropriate daily body weight (N) of each individual.

When integrating velocity from force, one must account for the missing constant of integration. For locomotion at constant speeds, this is achieved by assuming that the vertical integration constant is zero over an integral number of strides and estimating the horizontal integration constant using the average horizontal velocity measured by other means (Heglund et al., 1982). As with any movement initiation, an animal must be accelerating during take-off and, since take-off is a singular event that does not return the center of mass to the same vertical location, neither of these assumptions is appropriate to the current study. Thus, another method of calculating velocities must be used.

At the instant at which the center of mass reverses direction (i.e. stops downward movement and starts moving upwards), vertical velocity calculated from kinematic data is zero. I determined the time of this reversal in each trial and corrected the velocity calculated from the force platform data to be zero at that time. The horizontal integration constant was estimated as the pre-take-off horizontal velocity calculated from the kinematic data. Using this approach, when force data are integrated twice to calculate position, the position *versus* time plots from each source match inflection points.

Kinematics

Marker positions in all trials were digitized using Peak5 (v. 5.0.7; Peak Performance Technologies). Reference marks at each end of the force plate were used to set the scale for

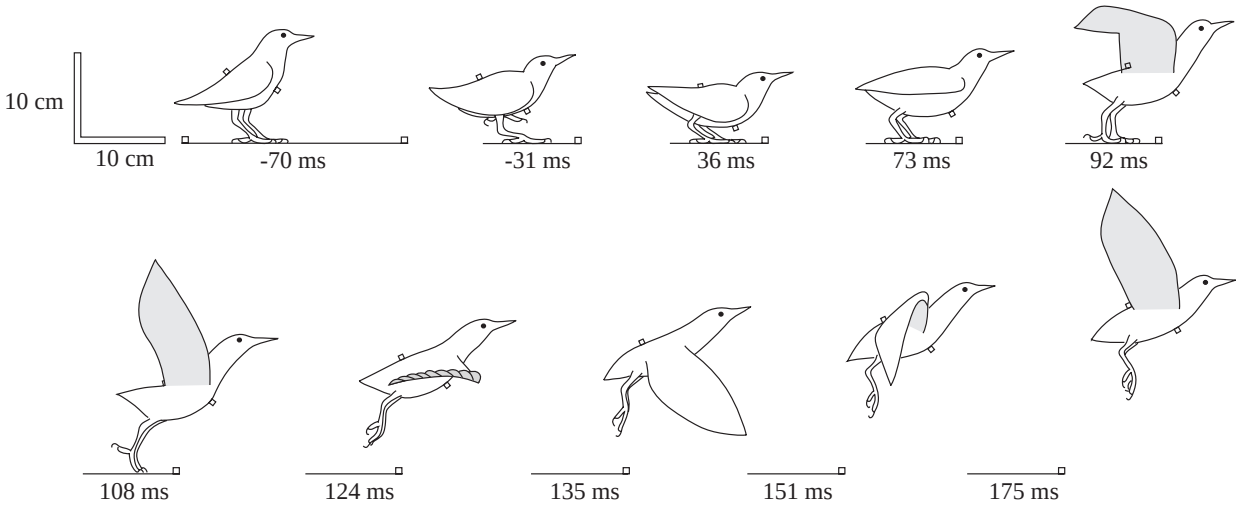

Fig. 3. *Sturnis vulgaris* body position during take-off. Sketches from video recordings (1001 frames s^{-1}) represent key events in the take-off sequence and are not evenly spaced frames. Time notations (ms) are relative to the defined start of take-off (vertical force >105 % of body weight). The horizontal bar under the first sketch represents the force plate surface. In subsequent pictures, the marker at the right-hand end of the force plate is maintained as a reference point. Events: standing position (–70 ms); mid-countermovement (–31 ms); end of countermovement/start of take-off (36 ms); wings begin unfolding (73 ms); wings half-unfolded/'heel'-off (92 ms); start of downstroke/lift-off (108 ms); mid-downstroke (124 ms); downstroke/upstroke transition (135 ms); mid-upstroke (151 ms); upstroke/downstroke transition/end of take-off (175 ms).

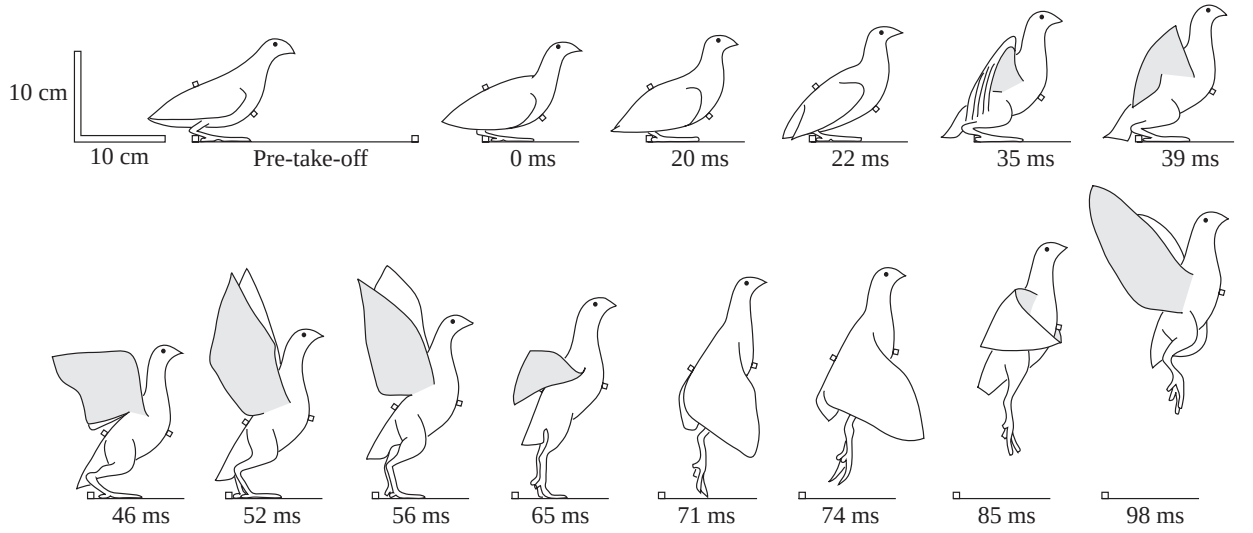

Fig. 4. *Coturnix coturnix* body position during take-off. Conventions as in Fig. 3, but the marker at the left-hand end of the force plate is maintained as a reference point. Events: pre-take-off body position; start of take-off (0 ms); one-third body rotation (20 ms); wings begin unfolding (22 ms); wings half-unfolded (35 ms); start of center of mass upward movement (39 ms); wings three-quarters unfolded (46 ms); start of downstroke (52 ms); 'heel'-off (56 ms); mid-downstroke (65 ms); lift-off (71 ms); downstroke/upstroke transition (74 ms); mid-upstroke (85 ms); upstroke/downstroke transition/end of take-off (98 ms).

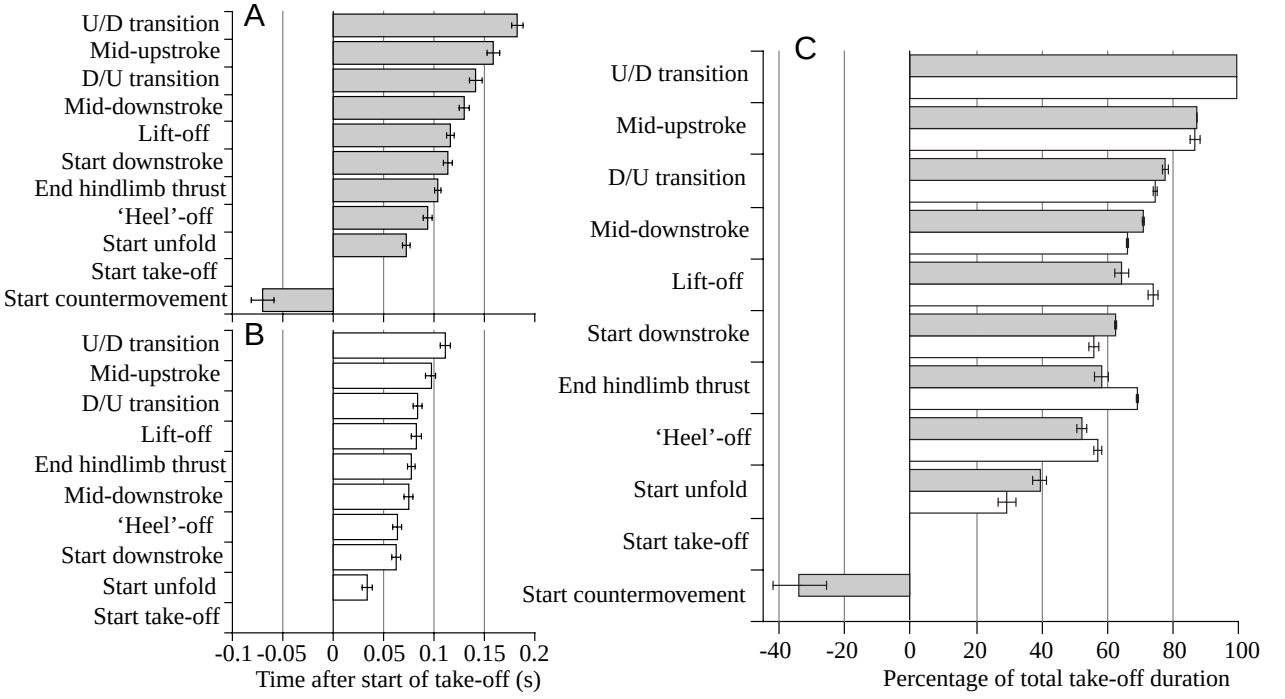

Fig. 5. Timing of take-off events. All bars represent mean ± S.E.M. The same events are represented but the order of events differs between (A) *Sturnis vulgaris* (*N*=3) and (B) *Coturnix coturnix* (*N*=3). (C) Species comparison. Events are ordered on the *y*-axis as in A, but bars are presented as a percentage of total take-off duration rather than as absolute time. D/U transition, downstroke/upstroke transition; U/D transition, upstroke/downstroke transition.

kinematic calculations and to align the origins of all captured video frames. Significant events during take-off (e.g. foot contacts, wing opening, wing cycle events) were noted relative to the analog trigger output.

All video frames from each trial were used in kinematic calculations. To minimize the effects of digitizing error, I applied a polynomial curve fit to all position data. Raw residuals from the curve fit varied by a maximum of ±1.5 mm, which is within the size range of the digitizing markers. Smoothing reduced this variation to less than 0.5 mm.

Smoothed residuals were re-added to the fitted curves, and the resulting data were used to calculate velocities and angles.

Some digitizing markers were covered during portions of a trial, usually by the wing. Missing data were estimated by linear interpolation over the entire data range, and the interpolated data were used as the source for the polynomial curve fits. For regions outside these gaps, interpolation did not modify the data.

Velocity was calculated as the derivative of the position of each marker; only those calculated for the center of mass are reported here. Impulse (N s) was calculated from the position data as the individual body mass (kg) times instantaneous velocity (m s^{-1}). Impulse was then converted to a multiple of body weight ($\times m\boldsymbol{g}$ s).

Three angles were defined to describe body movements during take-off (Fig. 2B). Body angle was defined as the angle between a line joining the synsacrum and breast markers and the horizontal; this angle approaches zero as the body axis becomes more vertical. The intertarsal angle (IT) was defined by the positions of the tibiotarsus, distal tibiotarsus and distal tarsometatarsus markers. The tarsometatarsus angle (TMT) described the angle between the tarsometatarsus and the ground, and was defined by the positions of the proximal and distal tarsometatarsus markers.

Results

Kinematics

In *S. vulgaris* take-offs, the animal moves from a standing position into a crouch, lowering its center of mass (Fig. 3, −70 to 36 ms). After the lowest point of the crouch, the breast swings forward and the hindlimbs extend, starting to raise the center of mass; the wings remain folded against the body (Fig. 3, 36–73 ms). The wings begin to unfold soon afterwards, reaching full extension and starting the downstroke approximately 45 ms later (Fig. 3, 108 ms). The entire take-off sequence, including time for the countermovement, averages 245±15 ms (mean ± S.E.M., *N*=3 individuals). If the countermovement is excluded, *S. vulgaris* take-off averages 183±5 ms (*N*=3).

C. coturnix take-offs start with the bird in a squatting position (Fig. 4). Prior to the start of take-off, the feet lift quickly and reposition parallel to each other, without visible countermovement. Following this repositioning of the feet, the body rotates, swinging the breast forward and up (Fig. 4, 0–22 ms). The wings start to unfold in the middle of this rotation and reach full extension approximately 30 ms later (Fig. 4, 52 ms). The hindlimbs extend as the wings unfold, pushing the bird upwards. Downstroke begins near the time at which the animal lifts the distal end of the tarsometatarsus from the ground and elevates the hallux to roll forward onto the middle and anterior phalanges (hereafter referred to as 'heel'-off). The wings are between mid-downstroke and the end of downstroke at lift-off, with the hindlimbs fully extended (Fig. 4, 71 ms). The entire take-off takes 111±5 ms (*N*=3).

Except for the start of wing unfolding, all forelimb events in *S. vulgaris* occur at the same time as, or subsequent to, lift-off; downstroke starts at the time the feet leave the ground (Fig. 5A). Downstroke in *C. coturnix* occurs at the time of 'heel'-off, while lift-off corresponds with the downstroke/upstroke transition (Fig. 5B). The animal is at mid-downstroke at the end of hindlimb thrust. Normalizing for take-off time, *S. vulgaris* and *C. coturnix* take-off events occur in a different order (Fig. 5C). *C. coturnix* lift off relatively later in the take-off, but start unfolding their wings earlier. In general, *C. coturnix* hindlimb movements occur later in the take-off than those of *S. vulgaris*, while their wing movements begin earlier.

Because of its initial countermovement, *S. vulgaris* starts

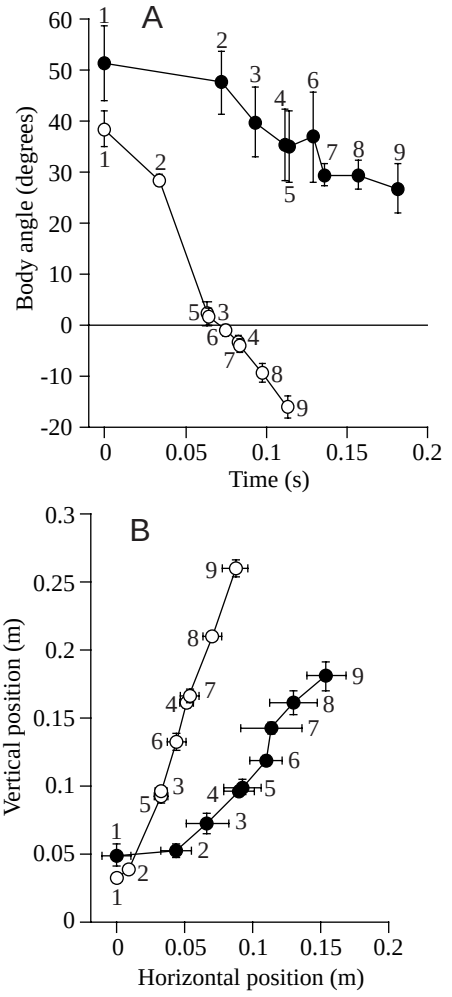

Fig. 6. Comparison of body kinematics. Filled circles represent *Sturnis vulgaris*, and open circles represent *Coturnix coturnix*. (A) Body angle. (B) Center of mass position as determined from kinematics. For comparison, the horizontal position is set to zero at the start of take-off in both species. In both plots, the numbers next to the markers indicate events from Fig. 5: 1, start of take-off; 2, start of wing unfolding; 3, 'heel'-off; 4, lift-off; 5, start of downstroke; 6, mid-downstroke; 7, downstroke/upstroke transition; 8, mid-upstroke; 9, upstroke/downstroke transition/end of take-off. Note that the order of the numbers reflects the different sequence of events in the two species. Refer to Figs 3 and 4 for body position. All points represent mean ± S.E.M. (*N*=3).

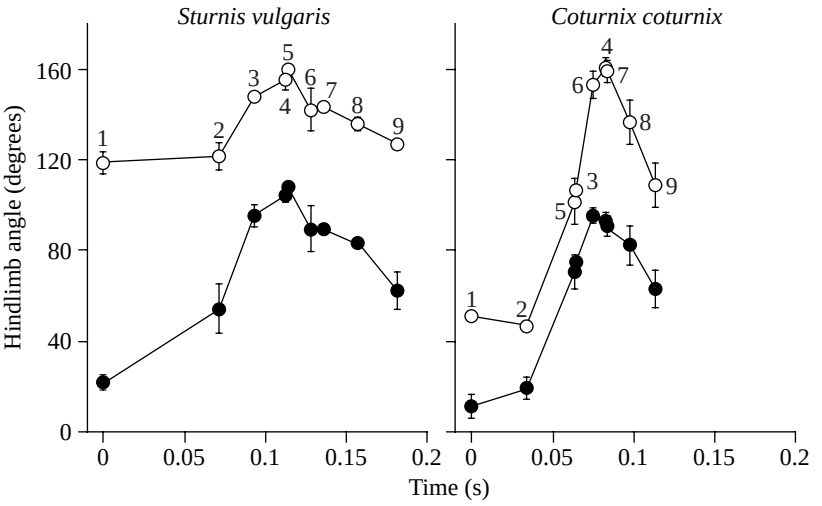

Fig. 7. Hindlimb angles during take-off. Open symbols in both plots show intertarsal (IT) angle, and filled symbols show tarsometatarsus (TMT) angle. Point numbering as in Fig. 6. All points represent mean ± S.E.M. (N=3).

take-off with a greater body angle than *C. coturnix* (Fig. 6A, point 1). When the wings begin to unfold, *S. vulgaris* has not changed orientation significantly, while *C. coturnix* has rotated the body 10 ° vertically (Fig. 6A, point 2). Body rotation in *C. coturnix* continues until, at 'heel'-off, the body angle is nearly zero (Fig. 6A, point 3). The overall body rotation of *S. vulgaris* is smaller, reaching only 35 ° at lift-off (Fig. 6A, point 4). Body rotation continues in *C. coturnix* after lift-off, and take-off ends with a body angle of −18 ° (Fig. 6A, points 7–9). The body is completely vertical at the end of take-off (Fig. 4, 98 ms). *S. vulgaris* stops body rotation with lift-off, and maintains the same axis position until the end of take-off (Fig. 6A, points 7–9; Fig. 3, 124–175 ms). Overall, take-off trajectory is more vertical in *C. coturnix* (Fig. 6B).

While the countermovement gives *S. vulgaris* a greater body angle at the start of take-off, *C. coturnix* is more crouched (i.e. shows greater hindlimb flexion; Fig. 7, point 1). The initial intertarsal (IT) and tarsometatarsus (TMT) angles are smaller than in *S. vulgaris*. In both species, IT angle remains constant until the wings begin to unfold, while TMT angle increases (Fig. 7, point 2). Thus, the first movement of the hindlimbs appears as dorsiflexion at the metatarso-phalangeal joint, with no extension of the IT joint. At 'heel'-off in both species, the tarsometatarsus is nearly vertical (90 °) and at approximately 80 % of its maximum position (Fig. 7, point 3). At the same instant, the *S. vulgaris* IT joint is approximately 90 % extended, while the *C. coturnix* joint is only at 66 % extension. Both species reach maximum IT and TMT extension at lift-off (Fig. 7, point 4); the angles then decline as the hindlimbs fold closer to the body (Fig. 7, points 7–9).

Mechanics

In *S. vulgaris*, maximum vertical and horizontal force reach 4.0 and 1.5 times body weight, respectively. *C. coturnix* produces vertical forces of 7.8 times body weight and horizontal forces of 2.8 times body weight (Table 1). Both weight-normalized vertical and horizontal maximum force magnitudes differ significantly between species (nested analysis of variance, ANOVA, Table 2, Species). Variation in force production within species, while significant for horizontal force [Table 2, Individual (species)], is less than the difference between species.

Table 1. *Maximum force production during take-off*

		Vertical		Horizontal	
	N	N	×mg	N	×mg
Sturnis vulgaris	3	3.09±0.04	4.04±0.22	1.13±0.12	1.48±0.16
Coturnix coturnix	3	13.10±0.21	7.80±0.19	4.73±0.33	2.82±0.21

Values are presented as absolute values (N) and as a multiple of body weight (×mg), where m is body mass in kg and g is the acceleration due to gravity, and means ± S.E.M.

Vertical force is generated and declines much more rapidly in *C. coturnix* than in *S. vulgaris* (Fig. 8). Both species generally show a decrease in vertical force prior to the start of take-off (time zero, Fig. 8), but kinematic analysis shows that only *S. vulgaris* performs a countermovement (see above). The start of take-off marks the end of this countermovement and is the time at which the body stops moving downwards.

Horizontal force production reaches a maximum early in *C. coturnix* take-off, at approximately the time at which the wings

Table 2. *Force: results of nested analysis of variance*

		d.f.	MS	F	P
Vertical	Species	1	140.46	171.09	0.0002
	Individual (species)	4	0.82	2.51	0.0599
	Residual	34	0.33		
Horizontal	Species	1	17.83	25.72	0.0071
	Individual (species)	4	0.69	4.47	0.0052
	Residual	34	0.16		

d.f., degrees of freedom; MS, mean square.

Table 3. *Maximum velocity during take-off calculated from force plate data and kinematics*

		Vertical		Horizontal	
	N	From force data	Total	From force data	Total
Sturnis vulgaris	3	1.36±0.10	1.47±0.05	1.19±0.07	1.48±0.02
Coturnix coturnix	3	3.31±0.07	3.75±0.06	1.23±0.11	1.18±0.10
		Pre-lift-off	Mid-downstroke	Lift-off	D/U transition

Values are means ± S.E.M.
D/U, downstroke/upstroke.

unfold (Fig. 8B, dashed arrow). There is a second maximum near the time of 'heel'-off corresponding in relative magnitude and timing to the horizontal maximum force produced in *S. vulgaris* take-off (Fig. 8B, 'H'). At the time of maximum horizontal force production in *C. coturnix*, the body has completed approximately one-third of its total rotation (Fig. 6A, point 2), although the center of mass has not moved far from its original position (Fig. 7, point 2).

Relative to total take-off duration, maximum vertical force production occurs at the same time in both species, but maximum horizontal force generation occurs earlier in *C. coturnix* (Fig. 9, 'H'). The timing of force generation relative to the actions of the wings differs significantly between species; the wings of *C. coturnix* begin to unfold prior to the vertical force maximum (Fig. 9, 'V'), while *S. vulgaris* starts unfolding its wings near the time of maximum vertical force generation. Unfolding of the wings uses approximately the same proportion of take-off duration in both species, but downstroke takes relatively less time in *S. vulgaris*. The total hindlimb force production duration (from the start of take-off until lift-off) is also relatively longer in *C. coturnix*.

Through a combination of greater relative hindlimb force production and relatively longer contact time, *C. coturnix* generates greater vertical impulse with the hindlimbs than does *S. vulgaris*. Maximum vertical velocity calculated from the force plate data (Fig. 10, blue lines) is thus greater in *C. coturnix*;

Table 4. *Velocity: results of nested analysis of variance*

		d.f.	MS	*F*	*P*
Vertical	Species	1	2.59	492.01	0.0001
	Individual (species)	4	0.05	1.98	0.1247
	Residual	34	0.03		
Horizontal	Species	1	0.66	2.52	0.0631
	Individual (species)	4	0.10	2.54	0.0611
	Residual	34	0.04		

d.f., degrees of freedom; MS, mean square.

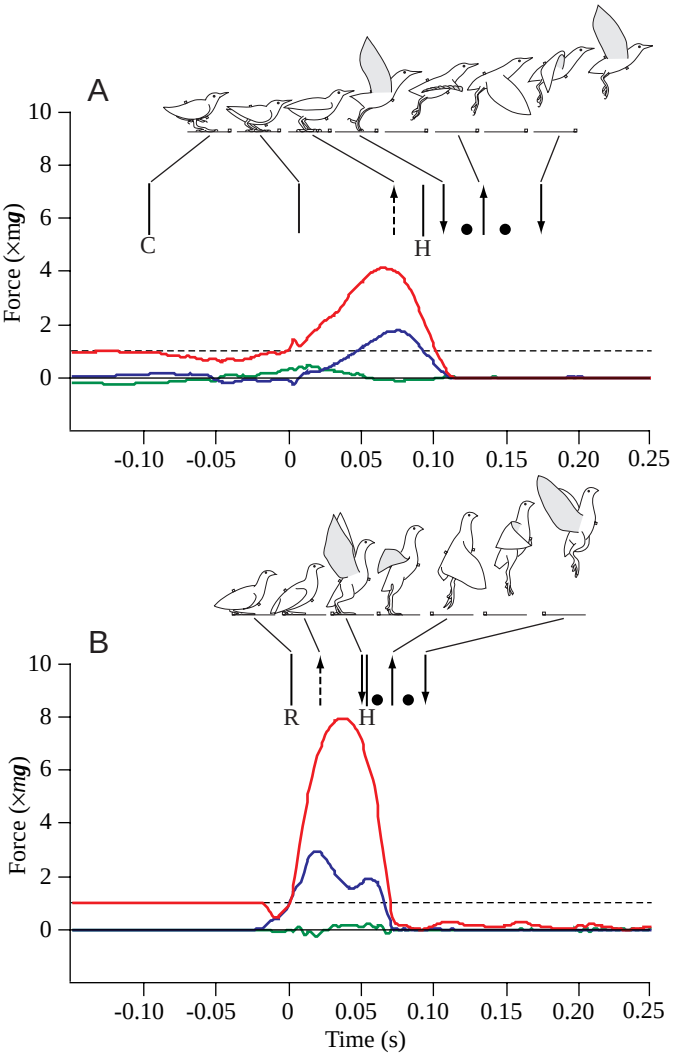

Fig. 8. Force platform output (as a multiple of body weight; ×*mg*, where *m* is mass in kg and ***g*** is the acceleration due to gravity) for a representative trial from each species. (A) *Sturnis vulgaris*. (B) *Coturnix coturnix*. Red lines are vertical force, blue are horizontal force and green are lateral force. C, start of countermovement in *S. vulgaris*; R, start of body rotation in *C. coturnix*; H, 'heel'-off. Arrows and filled circles indicate wing events: broken arrow, start of wing unfolding; downward-pointing arrow, start of downstroke and upstroke/downstroke transition; upward-pointing arrow, downstroke/upstroke transition. Filled circles represent mid-downstroke and mid-upstroke, respectively. See sketches above each plot for body position reference. The horizontal broken line indicates body weight.

3.3 m s^{-1} *versus* 1.4 m s^{-1} for *S. vulgaris* (Table 3). The partitioning of velocity generation during limb extension is also different between the species. At 'heel'-off, *C. coturnix* has produced only 89% of the total velocity produced by the hindlimb while *S. vulgaris* has generated 95% (Fig. 10, blue lines at 'H'). This indicates that 'heel'-off is not mechanically similar between the two species; *S. vulgaris* has essentially stopped producing acceleration with the hindlimb at a time when *C. coturnix* is still accelerating. Maximum vertical velocity is

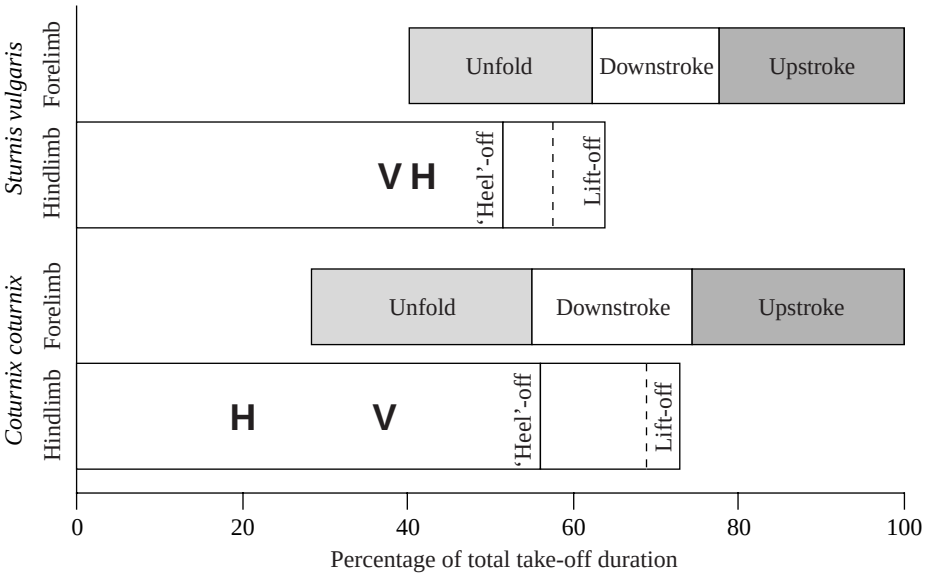

Fig. 9. Relative timing of the mechanics and kinematics for the two species. V, maximum vertical force production; H, maximum horizontal force production. The broken line indicates the end of hindlimb thrust.

achieved at mid-downstroke in both species (Fig. 10, first filled circle), but total vertical velocity is greater in *C. coturnix* (Fig. 10, red lines); 3.8 m s^{-1} *versus* 1.5 m s^{-1} for *S. vulgaris* (Table 3; nested ANOVA Table 4). This indicates that the wings of *C. coturnix* are producing lift (vertical force) prior to lift-off, adding to the force produced by the hindlimbs, while those of *S. vulgaris* accelerate the body only subsequent to lift-off.

Discussion

Previous work has suggested that the hindlimbs may be required during avian take-off to move the animal far enough away from its initial position to provide room for the wings to complete a full downstroke without hitting the substratum (Heppner and Anderson, 1985). It has also been proposed that the hindlimbs work to aid lift production during take-off, increasing airflow over the wings by running (Rüppell, 1975). Both hypotheses suggest that the wings are the primary lift and thrust generators during take-off; the hindlimbs are viewed as assisting the wings, implying that take-off could occur without them. However, neither of these studies considered take-off from the ground; Heppner and Anderson (1985) looked at take-off from a perch and Rüppell (1975) at take-off from water. Take-off from an elevated surface has more potential for mechanical and kinematic variability than take-off from the ground (see below) and, although take-off from the water is seen in many species, aquatic mechanics may not be applicable to more solid substrata. Thus, neither model provides clear information on the basic mechanics of take-off.

Marden (1987) showed that the hindlimbs are not required for take-off from the ground since, in the avian species he studied, hindlimb movement was constrained by the placement of weights. His experiments on insects, bats and birds did show that maximum lift production by the wings does not scale with body mass and that all animals showed failure to take off at similarly loaded flight muscle ratios [flight muscle mass/(body mass + added mass)]. Marden's experiments do not represent normal avian take-off mechanics and cannot be directly compared with the take-offs analyzed here. They do indicate, however, that during normal, unloaded take-off it is unlikely

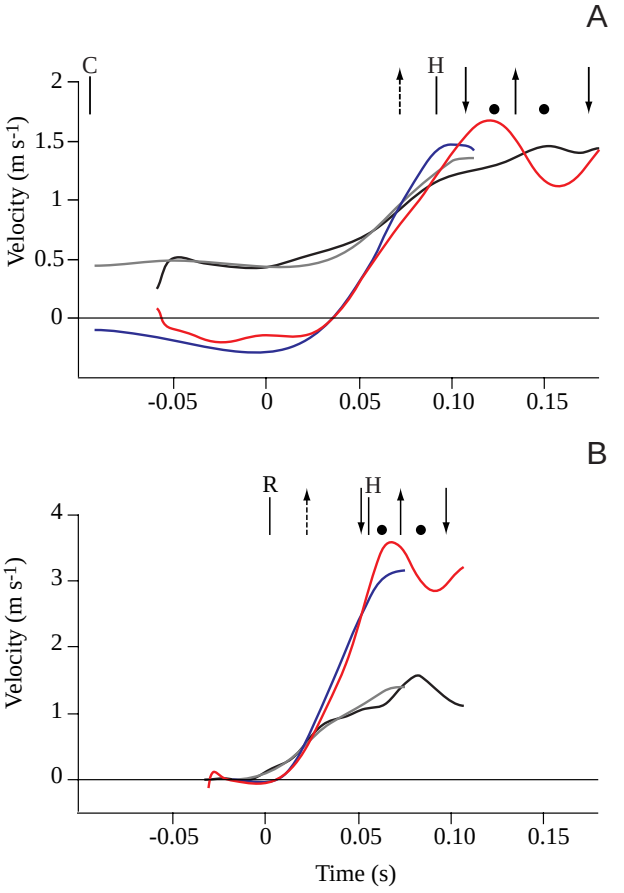

Fig. 10. Velocity (m s^{-1}) during take-off. (A) *Sturnis vulgaris*. (B) *Coturnix coturnix*. Red lines, total vertical velocity; blue lines, vertical velocity calculated from force data; black lines, total horizontal velocity; gray lines, horizontal velocity calculated from force data. Event markers above each plot are as in Fig. 8.

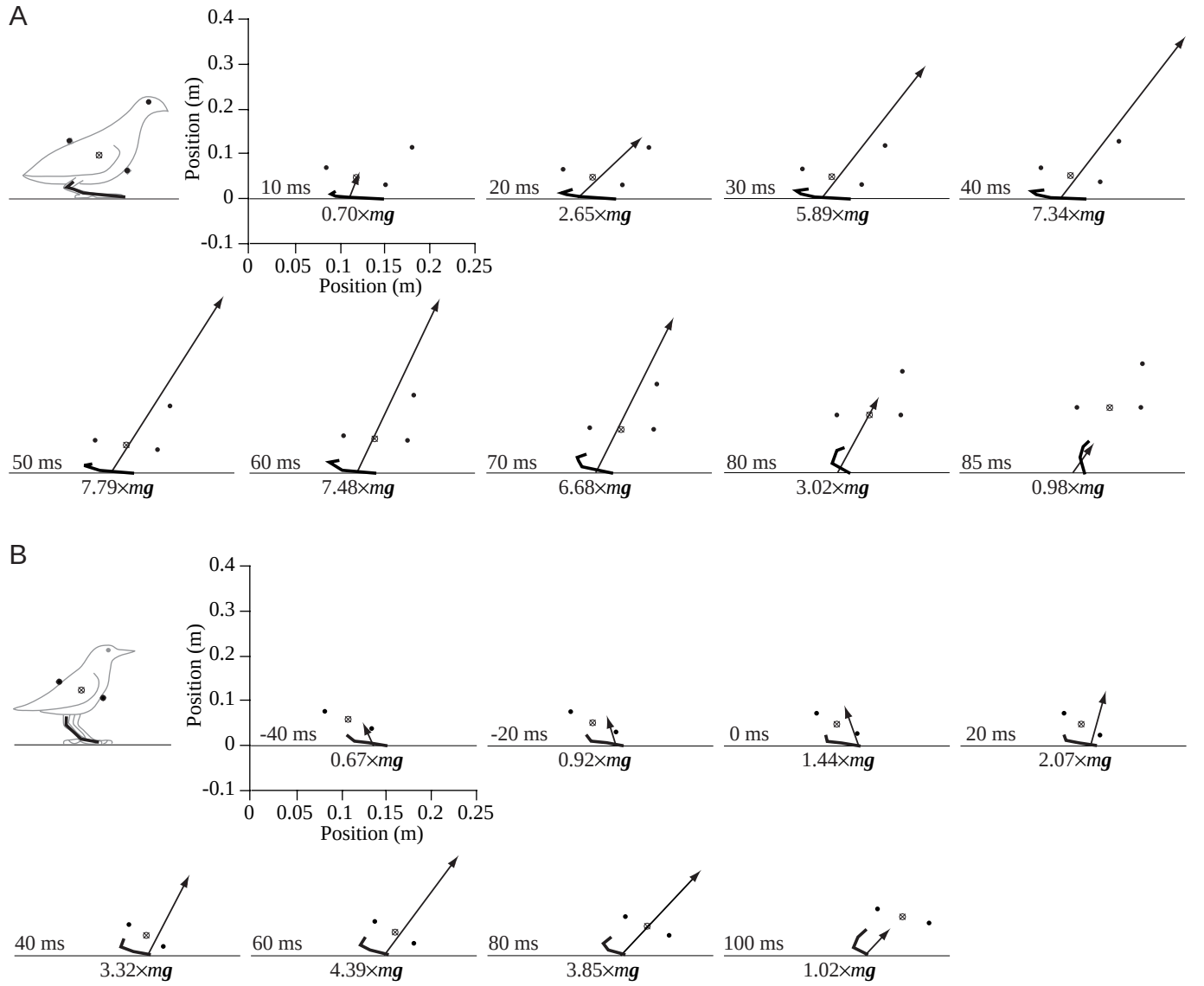

Fig. 11. Ground reaction force position, magnitude and direction, relative to digitized marker positions. Time notations are relative to the start of take-off. Numbers below axes indicate the magnitude of the ground reaction force in multiples of body weight, where *m* is body mass in kg and ***g*** is the acceleration due to gravity. (A) *Coturnix coturnix*. (B) *Sturnis vulgaris*.

that the wings of most species are producing maximum effort. The present study, through simultaneous analysis of the kinematic and mechanical aspects of avian take-off, shows that the hindlimbs are central to normal ground take-off.

Wing- or hindlimb-driven?

Given two possible power sources, the wings and the hindlimbs, and on the basis of morphological considerations and general locomotor habits, I hypothesized that *S. vulgaris* should use its wings to generate the majority of take-off velocity (Fig. 1A, wing-driven take-off) while *C. coturnix* should produce velocity primarily with the hindlimbs (Fig. 1B, hindlimb-driven take-off). Comparison of the velocity generated during *S. vulgaris* take-off (Fig. 10A) with these hypotheses shows that *S. vulgaris* performs hindlimb-driven take-off. Downstroke begins subsequent to maximum force production by the hindlimb (Fig. 8A). The impulse that can be attributed to the wings, and thus the velocity increase caused by lift and thrust, occurs only after this time (Fig. 10A). The hindlimbs produce 91 % of the total vertical velocity of take-off, while the first downstroke adds 9 % to the vertical velocity and provides 16 % of the total horizontal velocity (Table 3). Had it used only its wings, with the kinematics and mechanics seen here, *S. vulgaris* would have achieved a total velocity of only $0.24\,m\,s^{-1}$.

Take-off in *C. coturnix* is also hindlimb-driven. The velocity calculated from the force exerted on the plate accounts for 88 % of the total vertical velocity and 100 % of the horizontal velocity (Table 3). The wings, therefore, produce only 12 % of the vertical velocity and no thrust. The shape of the velocity trace and the timing of *C. coturnix* take-off loosely resemble those of the wing-driven hypothesis, with the wings starting

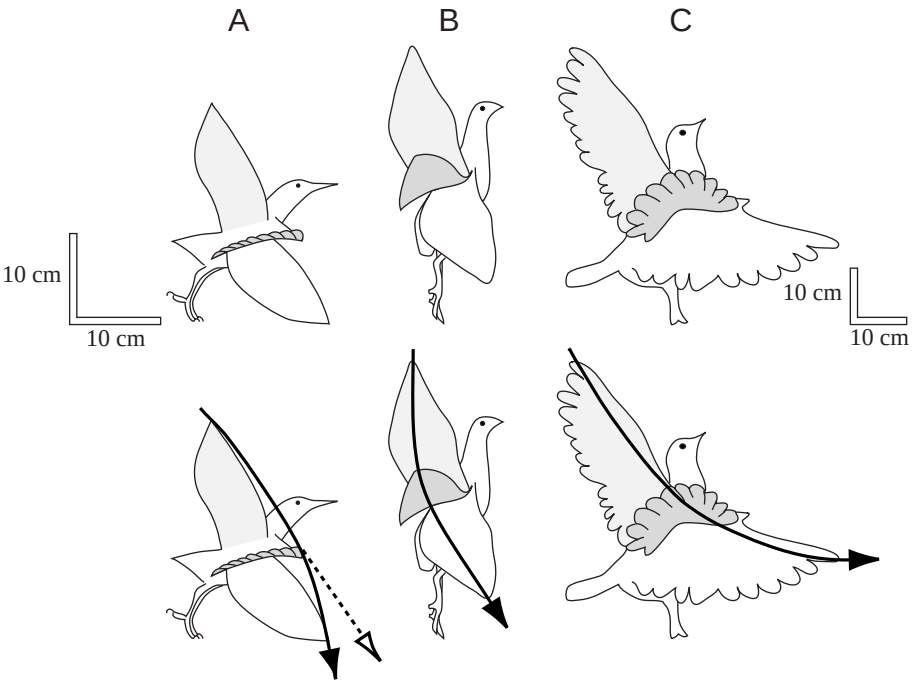

Fig. 12. Plane of the wingbeat during take-off for three species. The three wing positions represent the start of downstroke, mid-downstroke and the downstroke/upstroke transition; the body position is the position at lift-off. (A) *Sturnis vulgaris*. (B) *Coturnix coturnix*. Composite diagrams from Figs 3 and 4, respectively. (C) *Columba livia*. Modified from Simpson (1983). Left-hand scale for A and B, right-hand scale for C. The solid arrow represents the path of the wing tip during the downstroke. The broken arrow is a continuation of the path of the wing tip during the first half of the downstroke.

downstroke significantly before the peak of hindlimb-produced velocity (Fig. 10B). But the wing-driven hypothesis predicted that the contribution of the wings to take-off should be greater than that of the hindlimbs (Fig. 1B). The proportion of total velocity generated by the hindlimb refutes this hypothesis for *C. coturnix*; without the hindlimb, it would achieve a total velocity of only 0.44 m s^{-1}.

Force

Maximum vertical force production for *S. vulgaris* take-off was four times body weight (mean 4.0×$m\boldsymbol{g}$, range 2.8–5.3×$m\boldsymbol{g}$, N=3). This is higher than has been reported for *S. vulgaris* take-off from a perch (mean 2.6×$m\boldsymbol{g}$, range 1.4–3.9×$m\boldsymbol{g}$; Bonser and Rayner, 1996), indicating that ground take-off in this species entails greater muscular effort from the hindlimbs than take-off from an elevated perch. From an elevated surface such as a perch, gravity can assist take-off, allowing a bird to open its wings while falling to generate lift. The hindlimbs could generate sufficient force to move the bird forward from the perch before the wings are prepared to generate thrust, could produce the same force and acceleration as in ground take-off, or perch take-off could be accomplished with little or no hindlimb action. Therefore, animals taking off from a perch are likely to show greater variation in force magnitude, take-off trajectory and kinematics than animals performing ground take-off. Bonser and Rayner (1996) reported greater variation in ground reaction force angle from *S. vulgaris* during take-off from a perch (50–90 °; Bonser and Rayner, 1996) than I found in the present study (71.4±1.8 °; range 64.4–79.5 °, N=202). The higher variability in direction and the lower forces involved in perch-based take-off suggest that the overall mechanics and kinematics of these take-offs may be more variable than for take-off from the ground. The variation is likely, however, to be a modification of the pattern of ground take-off kinematics and mechanics.

Mean maximum vertical force production by *C. coturnix* was nearly eight times body weight (mean 7.8×$m\boldsymbol{g}$, range 7.2–8.6×$m\boldsymbol{g}$, N=3). Since both feet are in contact with the ground during the entire take-off, each foot is generating approximately four times body weight in vertical force. These single-leg forces are similar to the total two-leg forces recorded for *C. coturnix japonica* jumping over a 15 cm barrier (3.9×$m\boldsymbol{g}$; Clark and Alexander, 1975). Clearly, in this species, take-off entails significantly greater force generation than jumping over a low wall. Total vertical force production during take-off in *C. coturnix* is similar to that of the vampire bat *Desmodus rotundus* (Schutt et al., 1997). *D. rotundus*, using the forelimb as the primary accelerator, produced maximum vertical take-off forces of 6.5 times body weight (means ± S.D., 6.51±1.57×$m\boldsymbol{g}$, range 4.50–9.58×$m\boldsymbol{g}$; body mass 23.1±3.6 g, range 19.1–30.1 g, N=12; Schutt et al., 1997). The duration of force production by the bat is similar to that for *C. coturnix* (70±12 ms, mean ± S.D., N=12, Schutt et al., 1997; 83±2 ms, mean ± S.E.M., N=3, *C. coturnix*), although the shape of the force trace is substantially different. In the take-off of *D. rotundus*, there is a distinct plateau and ‘shoulder’ subsequent to maximum vertical force, which the authors associate with the sequential activation of the forelimb and pollical muscles, respectively. For both my study species, the vertical force curve is parabolic (Fig. 8). While sequential muscle activation within the hindlimb is likely, there is no obvious signature of it as in *D. rotundus*.

In force signature and overall mechanics, take-off in both study species is most similar to jumping. However, in this context, the symmetrical shape of the vertical force trace in *C. coturnix* is unusual. In *S. vulgaris*, the slope of the ascending

leg of the vertical force trace is half that of the descending leg; for *C. coturnix*, the ascending and descending legs have the same slope. The trace for *S. vulgaris* is more similar to force production seen in the jumps of anurans, cats and humans (see, for example, Zajac, 1985; Harman et al., 1990; Anderson and Pandy, 1993; Marsh, 1994). The symmetrical vertical force signature emphasizes the rapid nature of *C. coturnix* take-off and may be seen in future studies of species with similarly explosive take-off (e.g. other gallinaceous birds).

Body rotation

Both *S. vulgaris* and *C. coturnix* show significant body rotation during take-off. *C. coturnix*, starting in a crouch with the body angled at approximately 38 ° to the horizontal (Fig. 4, 0 ms; Fig. 6A, point 1), rotates the body almost vertically (body angle to 0 °) in the first 40 ms of take-off (Fig. 4, 39 ms; Fig. 6A, point 3/5). The body rotation of *S. vulgaris* is smaller, starting at approximately 50 ° (Fig. 3, −31 to 36 ms; Fig. 6B, point 1) and changing, by lift-off, to approximately 35 ° (Fig. 3, 108 ms; Fig. 6B, points 4/5).

In both species, the ground reaction force vector is oriented anterior to the center of mass for the first half of take-off (Fig. 11); the moment of this ground reaction force about the center of mass will act to decrease the body angle. While this rotating force acts for the same period in both study species, it produces different results. The forces generated by *C. coturnix* are twice as large as those produced by *S. vulgaris*, logically leading to the greater rotation seen in *C. coturnix*. Also, in *C. coturnix*, the horizontal force peak prior to maximum vertical force keeps the ground reaction force angled anteriorly throughout take-off, a pattern different from that in *S. vulgaris*, in which the ground reaction force is initially directed posteriorly. Finally, the countermovement of *S. vulgaris* imparts forward and downward momentum at the start of take-off. The initial ground reaction force near the start of take-off is vertical, rotating the body because of its position anterior to the center of mass, but primarily acting to slow and redirect the body's momentum (Fig. 11B, −20 to 0 ms). The body continues moving forward and, in the latter half of take-off, horizontal force production increases, directing the ground reaction force through the center of mass and moving the body upwards (Fig. 11, 60–100 ms). Body rotation in *S. vulgaris* is smaller than it might otherwise be because the anteriorly directed ground reaction force is used early in take-off to slow and reverse the downward momentum of the body, rather than purely for rotation as in *C. coturnix*.

At the conclusion of this experiment, I questioned whether the differences in mechanics between *C. coturnix* and *S. vulgaris* could be the result of the different trajectories at which the species were taking off. Increased force production and the earlier action of the wings in *C. coturnix* are logically associated with its nearly vertical take-off. To address this concern, a further experiment was performed that examined in more detail the take-off of *S. vulgaris* and tested whether the mechanics and kinematics of *S. vulgaris* take-off become more similar to those of *C. coturnix* at similar take-off trajectories (K. D. Earls, in preparation). Birds were trained to take off at higher trajectories, the highest of which was the same as that of the *C. coturnix* take-offs presented here. The mechanics of *S. vulgaris* take-offs do not alter to become like those of *C. coturnix* at high trajectory, confirming that the results presented here are differences between the species, not solely the result of take-off trajectory.

Scaling considerations

On the basis of mass alone, the take-off of *S. vulgaris* should be more rapid than that of *C. coturnix* (Bennet-Clark, 1977). In spite of the fact that *C. coturnix* has twice the body mass of *S. vulgaris*, its take-off occurs in half the time. In part, this difference may be due to differences in muscle composition between the two species; *S. vulgaris* has primarily red muscle while *C. coturnix* muscle is predominantly white (K. D. Earls, personal observation). The total hindlimb proportions of these two species also differ significantly. From measurements of the bones of museum specimens, *S. vulgaris* has a mean hindlimb length of 97.2±2.9 mm, while *C. coturnix* averages 104.4±1.7 mm (mean ± S.E.M., N=5). As noted above, the distal elements make up a greater proportion of the limb of *S. vulgaris*, while *C. coturnix* has a relatively long femur. In combination with larger gastrocnemius and thigh muscle masses in *C. coturnix*, this difference in limb proportions should alter the relative moments generated by the hindlimb. However, without more detailed analysis of the total movement of the hindlimb, possible only using X-ray, the actual influence of limb proportions on the take-off mechanics of *S. vulgaris* and *C. coturnix* is not predictable.

Size, limb proportions and muscle mass distribution may not be sufficient predictors of how take-off mechanics and kinematics will scale with body mass in birds because aerodynamics cannot be ignored. For example, the relatively longer distal elements in the forelimb of *S. vulgaris* and the wing's longer absolute unfolding time may determine a minimum duration for take-off in the species. Or, the fact that the wing is less cambered than that of *C. coturnix* may make it less efficient for lift generation at low airspeeds, constraining *S. vulgaris* to a hindlimb-driven take-off using relatively small hindlimbs.

Velocity and wing kinematics

In addition to the differences in hindlimb force production, the wing movements of the two species differ significantly. While aerodynamic models of flapping flight place maximum lift and thrust generation at mid-downstroke (Rayner, 1986), it appears that there may be partitioning of these forces during take-off in both *S. vulgaris* and *C. coturnix*. In both species, an increase in vertical velocity precedes the increase in horizontal velocity (Fig. 10, red and black lines). Vertical velocity begins to increase near the start of the downstroke (Fig. 10, downward arrow), while horizontal velocity begins to increase near mid-downstroke (Fig. 10, first filled circle), a pattern that suggests first lift and then thrust production during the downstroke.

During take-off, both study species added an average of 0.23 $m\,s^{-1}$ to their horizontal velocity between mid-downstroke and

the end of downstroke (Table 3). However, for *C. coturnix*, there is, on average, no difference between the horizontal velocity calculated from the kinematic analysis and from the force data. The observed increase in horizontal velocity can be directly attributed to hindlimb force generation. For *S. vulgaris*, the increase in horizontal velocity occurs after lift-off and must be generated by the wings. Therefore, during take-off as defined in this study, *C. coturnix* generates lift (vertical force) but not thrust (horizontal force) with the wings, and the wings of *S. vulgaris* generate both lift and thrust.

This difference in thrust generation may be attributed to the sweep of the wing relative to the body axis (Fig. 12). In *S. vulgaris*, the plane of the wingbeat is similar to that seen in forward flight (Rüppell, 1975; Tobalske and Dial, 1996), with the downstroke path of the wing tip nearly perpendicular to the antero-posterior axis of the body (Fig. 12A, solid line). In the second half of downstroke, the wing tip sweeps backwards rather than continuing the line of the first half of downstroke (Fig. 12A, broken line). The wing of *S. vulgaris* is therefore oriented to produce a vector force acting to move the center of mass forward. In contrast, the first wingbeat of *C. coturnix* is distinctly vertical, starting with the wing tip behind the head and ending with the wing covering the thigh and lower body (Fig. 12B). The wing is not oriented to produce an anteriorly directed force vector in the horizontal plane and seems to be primed to produce a posteriorly directed force, depending on the degree of body rotation.

One study from the literature provides another species for comparison. While the body attitude of the pigeons studied by Simpson (1983) is similar to that of *C. coturnix*, the orientation of the wing seems to be similar to that of *S. vulgaris*, relative to the body axis (Fig. 12C). However, connecting the wing tips gives a curve more similar to that of *C. coturnix*. This suggests that the pigeon may not produce forward thrust with the wing during take-off from the ground and may have take-off mechanics more similar to those of *C. coturnix*. Without synchronized measurements of kinematics and force production during ground take-off of *Columbia livia*, the exact mechanics will remain unclear.

Evolutionary implications

Flapping flight has been viewed as difficult to evolve directly in a terrestrial organism, largely because flight at low airspeeds is known to be energetically expensive (Pennycuick, 1975; Dial et al., 1997) and a gliding intermediate from an arboreal organism is aerodynamically simpler (Norberg, 1990). This view of flight evolution is based largely on modeling of the aerodynamic power required for flight, which produces a U-shaped curve; flight at low or high speeds requires a large amount of power, while at intermediate speeds there is a power output minimum at which flight is more efficient (Pennycuick, 1986; Rayner, 1986). Hypotheses of how flapping flight from the ground may have evolved in birds have focused on how a proto-flier could have achieved this minimum power speed and thus have started flapping flight at the least costly place on the power curve. These hypotheses have involved the proto-flier running along the ground with their wings outstretched and flapping shallowly, much like the take-off running of large waterfowl and albatross (Burgers and Chiappe, 1998; for review of cursorial theories, see Padian and Chiappe, 1998).

I propose that a cursorial-running model of avian flight evolution is unnecessarily complex. First, although flight at zero air speed is energetically costly, take-off is not the same as hovering; at no point during take-off are the wings moving to produce lift at zero airspeed. The present study shows that the body has some forward or upward velocity before wing movement; the wings of *S. vulgaris* do not begin the downstroke until the body is moving at approximately $1.25\,m\,s^{-1}$, while *C. coturnix* is moving at $2.5\,m\,s^{-1}$ before the first downstroke. Second, a running take-off of the type proposed in evolutionary hypotheses is seen in select groups of living birds that are morphologically specialized (e.g. albatrosses, loons), that are taking off from highly compliant surfaces (e.g. water) or are that are very large (e.g. swans). If the earliest flying forms or proto-fliers were more generalized in their habits or close to the average size of living birds, they may have performed like the majority of living birds and taken off from the ground without running. Finally, all the known fossil forms potentially related or ancestral to modern birds were bipedal, with upright hindlimbs. Not only is this hindlimb shape appropriate for cursorial behavior, it is ideal for jumping. Jumping is a mechanically simpler movement than running and is a method of reaching relatively high velocities in a short time. An animal performing a single jump followed by flapping is a simpler model for the evolution of take-off in early fliers and proto-fliers and has more support from the behavior of living birds than does a running model.

Jumping or leaping models of flight evolution have been proposed by Caple et al. (1983), on the basis of modeling of energy requirements, and more recently by Garner et al. (1999), looking at the sequence of character transitions in the avian lineage. These models of flight evolution are better supported by the mechanical analysis performed here than is a cursorial-running model, but I think we must consider a conceptual modification. I propose that a jumping model of flight evolution need not be linked to a specific behavior (prey capture), habitat structure (boulders or broken substratum, Garner et al., 1999) or energetic benefit (Caple et al., 1983). Given the hindlimb morphology of early avian ancestors, jumping was probably a common locomotor behavior. Both theoretically and practically, a model that adds a forelimb movement to a jump should not require the explanation of additional benefit, simply a lack of additional cost. Any downward movement of a feathered forelimb after the initiation of a leap could potentially add height or distance to the ballistic path, regardless of the reason for jumping. A jumping model of flight evolution also acts as a testable hypothesis for the evolution of supracoracoideus function in birds, since it immediately opens the door to selective pressure for a more rapid and larger-amplitude upstroke (Poore et al., 1997). All current models of flight evolution should be viewed as testable hypotheses, with mechanical analyses of the

locomotion of living birds designed as experiments to try to falsify those hypotheses.

Definition of take-off

If the wings were the primary take-off accelerator, the pectoralis and supracoracoideus muscle forces and power output should be high during take-off and potentially greater than those produced during level flapping flight, since the animal is accelerating. If the legs are the primary accelerators during take-off, as in *S. vulgaris* and *C. coturnix*, the muscles of the pectoral girdle may not show increased force production during take-off. Dial and Biewener (1993) measured pectoralis force output during many modes of flight of *C. livia* and defined take-off as including the first five wingbeats. They concluded that take-off, under their definition, involved as much pectoralis force output as vertical ascending flight (24.9±3.1 N for take-off *versus* 26.0±1.8 N for vertical ascending flight; means ± S.D., N=40). However, this conclusion depends on the definition of take-off. The pectoralis force output measured during the first two wingbeats was significantly lower than in those that followed and was within the same range as the force output during level flapping flight (level flapping flight, 19.7±2.0 N; mean ± S.D., N=40). The authors note: 'Since the legs thrust the bird upward during lift-off, the highest recordings of pectoralis force and EMG intensity... is observed during the second or third wingbeat' (Dial and Biewener, 1993; p. 41). In both my study species, the kinematics of the second wingbeat are different from that of the first, and by the third wingbeat *S. vulgaris* flight is not visibly distinguishable from level flight. These results, when combined, indicate that the transition from take-off to other modes of flight (level forward flight, vertical ascending flight, etc.) may happen more rapidly than has previously been thought.

Concluding remarks

The hindlimbs of *S. vulgaris* and *C. coturnix* produce the primary acceleration of take-off. The wings act either after the hindlimbs have finished producing force (*S. vulgaris*) or during the hindlimb action (*C. coturnix*), but in both species provide only 10–15 % of the total take-off velocity. The ground reaction forces produced during ground-based take-off are greater than any that have been recorded for perch-based take-off or for jumping in these species. Analyses of the ground take-off of other taxa is required, to include both a wider body size range and more diversity of body form, before more general patterns of take-off mechanics in birds will become clear.

With the narrower definition of take-off used in this study, where take-off includes all wing and body actions up until the upstroke/downstroke transition subsequent to the loss of contact with the substratum, ground take-off may not be as expensive in terms of wing force output as has been proposed from aerodynamic power calculations. This definition works for any take-off, whether it be a jumping take-off from the ground, a falling take-off from a moving tree limb or a running take-off from the water. While the present study does not address the question of how a proto-flier may have supported its body weight on small airfoils after take-off, I propose, on the basis of the available data from living birds, that flapping flight is not as difficult to evolve from a terrestrial, bipedal organism as has been previously supposed.

I gratefully acknowledge partial support of this project from NSF (IBN-9119413 to S. Swartz). I would like to thank Sharon Swartz, Stephen Gatesy, Jonathan Waage, Douglass Morse and two anonymous reviewers for their comments on the manuscript. I also thank G. E. (Ted) Goslow and Jessica Theodor for comments on the manuscript and technical assistance. Special thanks to Robert McGovern for technical aid far beyond the call of duty.

References

Alexander, R. McN. (1995). Leg design and jumping technique for humans, other vertebrates and insects. *Phil. Trans. R. Soc. Lond. B* **347**, 235–248.

Anderson, F. C. and Pandy, M. G. (1993). Storage and utilization of elastic strain energy during jumping. *J. Biomech.* **26**, 1413–1427.

Bennet-Clark, H. C. (1977). Scale effects in jumping animals. In *Scale Effects in Animal Locomotion* (ed. T. J. Pedley), pp. 185–201. New York: Academic Press.

Bonser, R. H. C. and Rayner, J. M. V. (1996). Measuring leg thrust forces in the common starling. *J. Exp. Biol.* **199**, 435–439.

Brown, R. H. J. (1948). The flight of birds: the flapping cycle of the pigeon. *J. Exp. Biol.* **25**, 322–333.

Burgers, P. and Chiappe, L. M. (1999). The wing of *Archaeopteryx* as a primary thrust generator. *Nature* **399**, 60–62.

Cabe, P. R. (1993). European Starling (*Sturnis vulgaris*). In *The Birds of North America*, No. 48 (ed. A. Poole and F. Gill), pp. 1–24. Philadelphia: The Academy of Natural Sciences.

Caple, G., Balda, R. P. and Willis, W. R. (1983). The physics of leaping and the evolution of pre-flight. *Am. Nat.* **121**, 455–467.

Clark, J. and Alexander, R. McN. (1975). Mechanics of running by quail (*Coturnix*). *J. Zool., Lond.* **176**, 87–113.

Dial, K. P. and Biewener, A. A. (1993). Pectoralis muscle force and power output during different modes of flight in pigeons (*Columba livia*). *J. Exp. Biol.* **176**, 31–54.

Dial, K. P., Biewener, A. A., Tobalske, B. W. and Warrick, D. R. (1997). Mechanical power output of bird flight. *Nature* **390**, 67–70.

Garner, J. P., Taylor, G. K. and Thomas, A. L. R. (1999). On the origins of birds: the sequence of character acquisition in the evolution of avian flight. *Proc. R. Soc. Lond. B* **266**, 1259–1266.

Gatesy, S. M. and Dial, K. P. (1993). Tail muscle activity patterns in walking and flying pigeons (*Columba livia*). *J. Exp. Biol.* **176**, 55–76.

Harman, E. A., Rosenstein, M. T., Frykman, P. N. and Rosenstein, R. M. (1990). The effects of arms and countermovement on vertical jumping. *Med. Sci. Sports Exerc.* **22**, 825–833.

Hartman, F. A. (1961). Locomotor mechanisms of birds. *Smith. Misc. Collns* **143**, 1–91.

Heglund, N. C., Cavagna, G. A. and Taylor, C. R. (1982). Energetics and mechanics of terrestrial locomotion. III. Energy changes of the centre of mass as a function of speed and body size in birds and mammals. *J. Exp. Biol.* **79**, 41–56.

Heppner, F. H. and Anderson, J. G. T. (1985). Leg thrust important in flight take-off in the pigeon. *J. Exp. Biol.* **114**, 285–288.

Johnsgard, P. A. (1988). *The Quails, Partridges and Francolins of the World*. Oxford: Oxford University Press.

Marden, J. H. (1987). Maximum lift production during takeoff in flying animals. *J. Exp. Biol.* **130**, 235–258.

Marsh, R. L. (1994). Jumping ability of anuran amphibians. *Adv. Vet. Sci. Comp. Med.* **38**B, 51–111.

Norberg, U. M. (1990). *Vertebrate Flight*. New York: Springer-Verlag.

Padian, K. and Chiappe, L. M. (1998). The origin and early evolution of birds. *Biol. Rev.* **73**, 1–42.

Pennycuick, C. J. (1975). Mechanics of flight. In *Avian Biology*, vol. 5 (ed. D. S. Farner and J. R. King), pp. 1–75. New York: Academic Press.

Pennycuick, C. J. (1986). Mechanical constraints on the evolution of flight. In *The Origin of Birds and the Evolution of Flight* (ed. K. Padian), pp. 83–98. San Francisco: California Academy of Sciences.

Poore, S. O., Sánchez-Haiman, A. and Goslow, G. E. (1997). Wing upstroke and the evolution of flapping flight. *Nature* **387**, 799–802.

Rayner, J. (1986). Vertebrate flapping flight mechanics and aerodynamics and the evolution of flight in bats. In *Bat Flight – Fledermausflug* (ed. W. Nachtigall), pp. 27–74. Stuttgart: Gustav Fischer.

Rüppell, G. (1975). *Bird Flight*. New York: Van Nostrand Reinhold Co.

Schutt, W. A. J., Altenbach, J. S., Chang, Y. H., Cullinane, D. M., Hermanson, J. W., Muradali, F. and Bertram, J. E. A. (1997). The dynamics of flight-initiating jumps in the common vampire bat *Desmodus rotundus*. *J. Exp. Biol.* **200**, 3003–3012.

Simpson, S. F. (1983). The flight mechanism of the pigeon *Columba livia* during takeoff. *J. Zool., Lond.* **200**, 435–443.

Tobalske, B. W. and Dial, K. P. (1996). Flight kinematics of black-billed magpies and pigeons over a wide range of speeds. *J. Exp. Biol.* **199**, 263–280.

Zajac, F. E. (1985). Thigh muscle activity during maximum-height jumps by cats. *J. Neurophysiol.* **53**, 979–994.